PORT SAID ENGINEERING RESEARCH JOURNAL
Port Said University - Faculty of Engineering

Volume 16 No. 1 pp: 1:11

EFFECT OF SECONDARY AIR ON THE FLOW FIELD INSIDE A GAS TURBINE COMBUSTOR

Ibrahim A.[*], *Nasser Shelil*[a] , *EZZ El-Dien A. H*[a] , *Mosleh M.*[b] *and Farag T. M.*[a]
[a] Mechanical Power Engineering Department, Faculty of Engineering, Port Said University, Egypt.
[b] Department. of Naval Architecture & Marine Engineering, Faculty of Engineering, Alexandria University, Egypt.

ABSTRACT

In the present work, the air flow pattern inside a gas turbine combustor is studied. The effect of primary air swirl, secondary to primary air ratio and secondary air direction on the flow field is investigated. For this purpose, a test rig was constructed including a vertical combustor provided with an air swirler, primary and secondary air lines. Four air swirlers having the same blockage ratio of 0.72 were used. The swirlers have different vane angles of 15º, 30º, 45º, and 60º which generate swirl numbers of 0.23, 0.50, 0.87 and 1.5, respectively. A three dimensional model was used to simulate the flow characteristics by using the computational fluid dynamics package Fluent 6.3. The measured and the calculated reverse flow zone sizes inside the combustor show a good agreement. Using the combustor with restricted end, the boundaries of the reverse flow zone for different swirl numbers up to 1.5, are performed completely inside the combustor. Increasing the swirl number, the size of the reverse flow zone is also increased in its length and width. Using the secondary air in tangential direction with secondary to primary air ratio of unity and swirl number of 0.87 produces minimum size of the reverse flow zone. The size of the reverse flow zone for forward direction is larger than that of backward one. Increasing the swirl number and the secondary to primary air mass ratio, the turbulence intensity level also increased. This level is higher for tangential direction than the other ones.

Keywords: Gas turbine combustor, Swirl number, Secondary air, Reverse flow zone and Recirculated mass flow ratio.
*Corresponding author. E-mail address: enfarag1611@yahoo.com.

ABBREVIATIONS

A/F	Primary air to fuel mass ratio
S	Primary air swirl number
SPAR	Secondary to primary air mass ratio
RFZ	Reverse flow zone
r/R	Dimensionless radial distance
x/D	Dimensionless axial distance

1 Introduction

Investigating the air flow pattern inside a gas turbine combustor is essential for complete understanding of the combustion process. The swirl of combustion air is very essential because it assists in flame stabilization. Swirl also improves flame stability as a result of the formation of recirculation zones [1]. The effect of swirl on the flow field has been studied by many investigators [1-7]. The swirl number (S) is the characteristic parameter of the swirl flow which is defined as the ratio between axial flux of the angular momentum to the axial momentum [1]. Chigier and Chervinsky [2] identified the critical swirl number to be of 0.6. In weak swirling flows (S<0.6), the axial pressure gradients are insufficient to cause internal recirculation of the flow. In strong swirling flows (S>0.6), strong radial and axial pressure gradients are set up near the swirler exit, resulting in a central recirculation zone. This recirculation zone constitutes a well mixed zone of combustion products and acts as a heat source that assists flame stabilization [3]. The air flow pattern inside a gas turbine combustor was investigated by El drainy et al.[4] using different swirlers. They concluded that the swirl number has a direct relationship with the size and shape of the central and corner recirculation zones. Buckley et al. [5] showed the effect of different swirlers on the combustor flow field and he used swirlers to enhance the performance of ramjet engines. Kilik [6, 7] demonstrated the effect of swirl vane

angle on the recirculation region and pressure drop downstream of the swirler. Nejad and Ahmed [8] and Ahamed and Nejad [9] presented measurements on the confined isothermal swirling flow by using two-component LDV system. They concluded that the swirler type as well as the swirl strength affect the flow field significantly Their results were used as database for numerical analyses.

Spatial velocity measurements were performed by Sheen et al. [10] for swirling flows with several swirl numbers by using LDV system. They concluded that the confinement ratio is an important parameter in swirl combustors.

Mathur and Maccallum [11] studied the enclosed swirling jet in a simplified model furnace. They found that velocity profiles are different from those obtained in free jets. Syred and Dahman [12] reported that the confinement ratio affect the aerodynamic flame shape, heat transfer and stability limits, especially when this ratio is less than 9.0 for swirl numbers greater than 0.5. These results were confirmed by Fu et al. [13] who executed a set of experiments and studied the effect of the confinement ratio on the aerodynamics of swirling flows using different test sections of confinement ratio of 4.6 to 18.5. They observed different modes for the recirculation zone depending on the confinement ratio, and they identified the critical confinement ratio to be 9.5.

Syred et al. [14] measured the temperature and velocity distributions in recirculation zones. They showed that under strong swirl, little change occurs to the flow fields as a result of the chemical reaction, the shape and size of the recirculation zone were slightly reduced compared with the isothermal conditions. They suggested that measurements in isothermal model would be sufficient to predict the size of the recirculation zone in case of combustion.

The effect primary air swirl number, and the interaction between the primary and normal directional secondary air on the flow field were examined by Attya et al. [15]. They concluded that increasing the total air flow rate increases slightly the size of the recirculation zone. The increase of the primary air swirl number increases both the size and intensity of the recirculation flow region. Also, a decrease in the secondary air ratio caused an increase in the recirculation zone size and intensity.

Tsioumanis et al., [16] developed a three-dimensional model to study the air flow pattern in an industrial burner. The air flow was split into primary and secondary air streams. Validation against experimental measurements as well as an investigation of the features in the air flow path was included. Also, Thundil K.R. and Ganesan V. [17] studied the swirling flow characteristics evaluated by the size of the recirculation zone and the mass trapped inside it. The standard k–ε model predicts the low swirl flow quite well and the RSM model predicts well the high swirl flows. The swirler with eight vanes and vane angle of 45^{o} is the best for producing appropriate recirculation zone for providing good flame stabilization characteristics.

From the previous literature studies, there is not enough data about the effect of the secondary air on the flow field in a gas turbine combustor. Secondary air is an important parameter used for cooling and dilution. The study of secondary air is essential for understanding the flow field and the combustion process. Therefore, in the present study, the effect of the secondary to primary air ratio and the secondary air inlet direction for different primary air swirl numbers is studied experimentally and theoretically. Validation of the calculation is done by comparing the CFD simulation results with the experimental ones. Four secondary air directions; normal, forward, backward and tangential directions are studied. The swirl number takes the values of 0.23, 0.50, 0.87 and 1.5. The effect of secondary air on the RFZ, the axial velocity distribution and turbulence in a gas turbine combustor will be investigated.

2- Experimental Test Rig

The schematic drawing of the test rig is shown in Fig.1. It includes a primary air line (11), a secondary air line (5) and a test combustor (14). A combustor of 20 cm inner diameter and 100 cm length was used. Two air blowers were used for supplying the primary and secondary air. Primary air is issued from blower (7), passes through an orifice (8), and enters the combustor through air swirler (13). The primary air flow rate is controlled by control valve (10) and is calibrated using an orifice (8) with a U-tube manometer (9). Secondary air is issued from air blower (1), passes through an orifice (3) and enters the secondary air inlet ports at the combustor periphery via flexible hoses (6). The secondary air flow rate is controlled by control valve (2) and is calibrated using an orifice (3) with a U-tube manometer (4**).**

Five combustors were used in the present study. A base combustor was constructed without secondary air and four combustors were constructed having secondary air inlets with different directions. Figure 2 shows the schematic drawing of the combustor shapes used in the study. Each combustor is equipped with 18 holes arranged along the combustor length. Secondary air inlets are arranged in four rows at equal distance of 10 cm and each row has four inlets. A pipe of 10 cm diameter (Figure 1) is fitted axially at the combustor up-stream inside which different swirlers could be mounted at its top. The burner assembly is shown in Fig. 3. The schematic drawing of the air swirler is shown in Fig 4. During tests, the primary air mass flow rate was

kept constant at 100 g/s (control valve was fully opened), while the secondary air mass flow rate was changed.

A flow direction detector probe is used to determine the boundaries of the RFZ [18,19]. The probe is connected to a pressure difference device TESTO 512 to measure the pressure difference between the two opposite holes. The points at which the pressure head difference changes its sign are detected and referred to the boundaries of the RFZ. The probe was inserted inside the combustor through the measuring ports, and was moved in radial direction till the device readings change its sign.

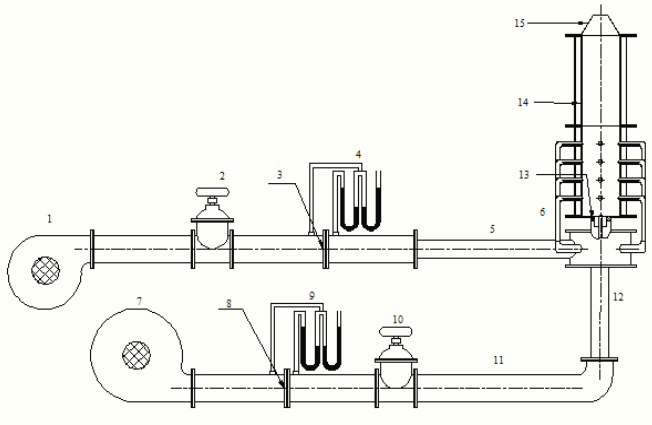

Fig. 1 Schematic drawing of the test rig

1	Secondary air blower	2, 10	Control valves	3, 8	Orifice-meters
4, 9	Water-tube manometers	5	Secondary air line	6	Flexible hoses
7	Primary air blower	11	Primary air line	12	Burner tube
13	Primary air swirler	14	Test combustor	15	combustor restricted end

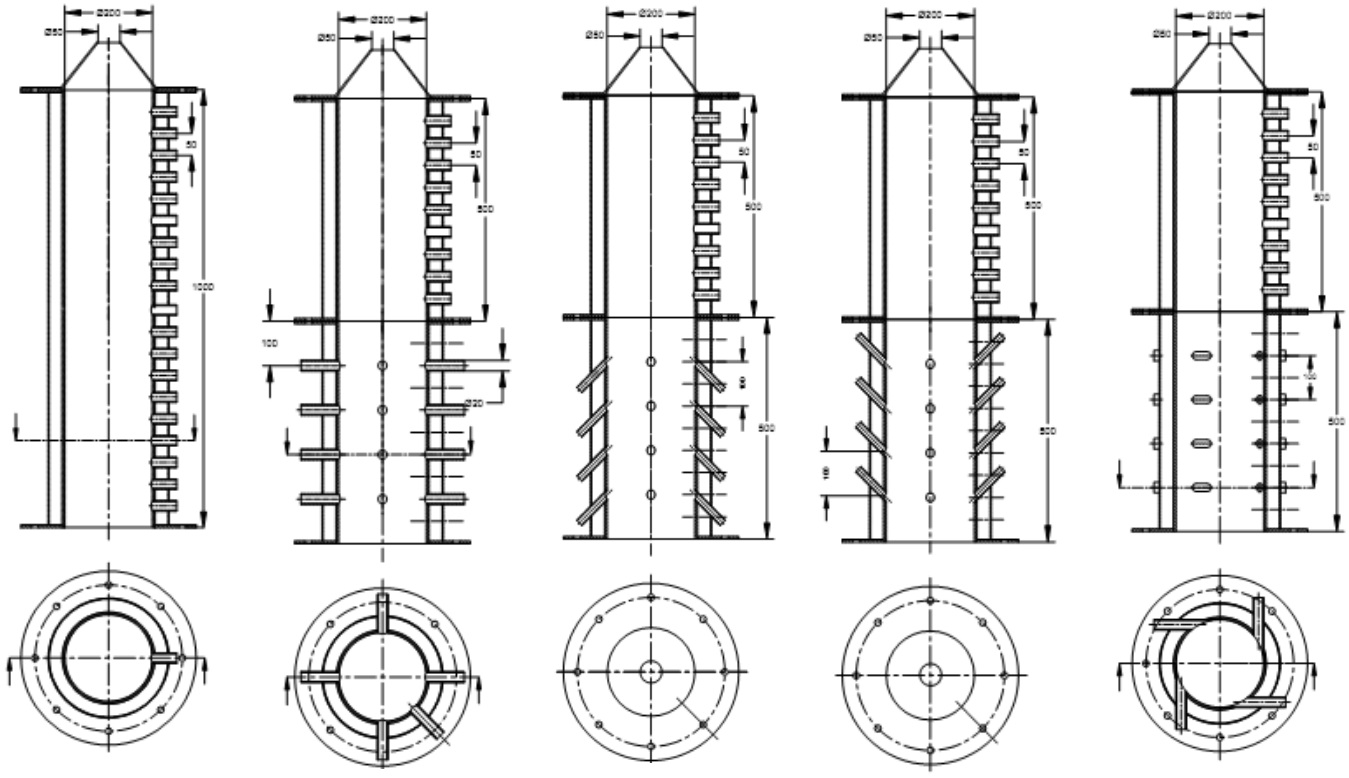

Base combustor Normal direction Forward direction Backward direction Tangential direction

Fig. 2 Schematic drawing of the combustor shapes (dimensions in mm)

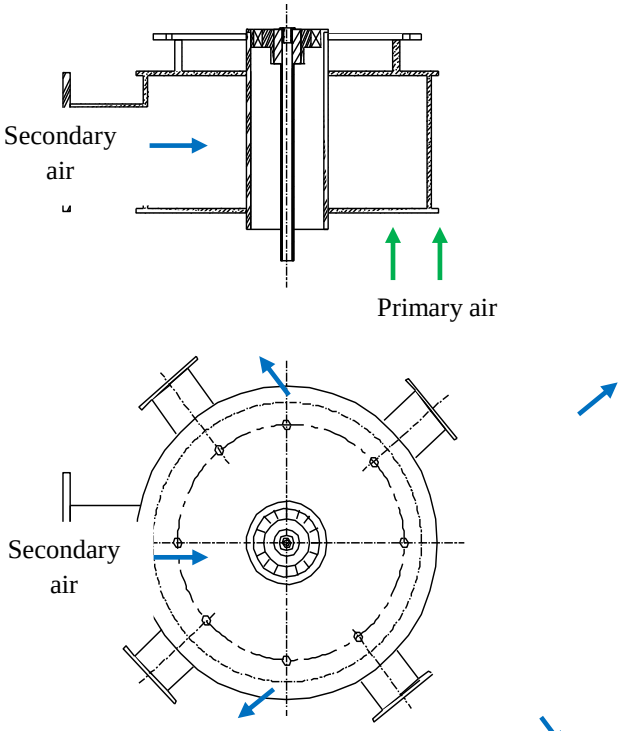

Fig.3 Burner assembly

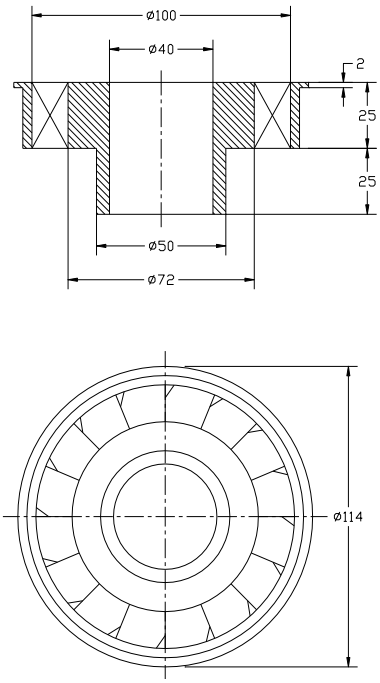

Fig. 4 Schematic drawing of the swirler (dimensions in mm)

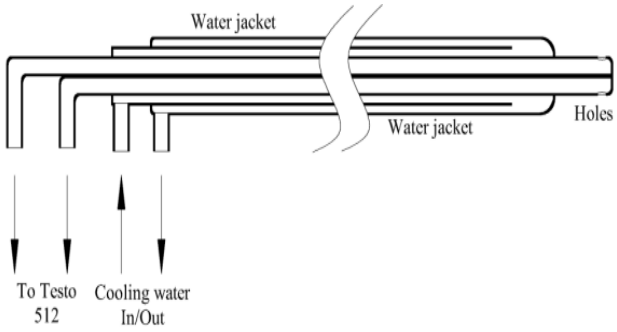

Fig 5 Assembly of the flow direction detector probe

3- CFD SIMULAION

The simulation of the cold flow field was performed using the computational fluid dynamics CFD code (Fluent 6.3) [20]. The model geometries were performed and meshes were generated for each swirl number using Gambit 2.3 preprocessing program [21]. The solutions were achieved and the results were displayed in Fluent 6.3. Figure 6 presents the computational grids for the 3D flows for swirl vane angle of 45° (S=0.87) and different secondary air directions.

The flow was assumed to be incompressible and turbulent. The governing equations are the conservation of mass and momentum. The most suitable turbulence model for simulating the swirl flow is the RSM model[22] but it requires higher computational efforts. The features of the k-ω model make it more accurate and reliable for a wider class of flows. Modifications are included so that the model equations behave appropriately in both the near-wall and far-field zones [20,23]. The SST k-ω model is utilized for the present simulations and the results obtained from that model indicate good agreement with the experimental data.

Fluent 6.3 uses a control-volume-based technique to convert a general scalar transport equation to an algebraic equation that can be solved numerically. This technique consists of integrating the transport equation about each control volume, yielding a discrete equation that expresses the conservation law on a control-volume basis. In the present case, the discretization of the governing equations is accomplished by using the first order upwind scheme. A steady state pressure based solver in fluent was used to solve the governing equations. This solver uses an algorithm which solves the governing equations consecutively.

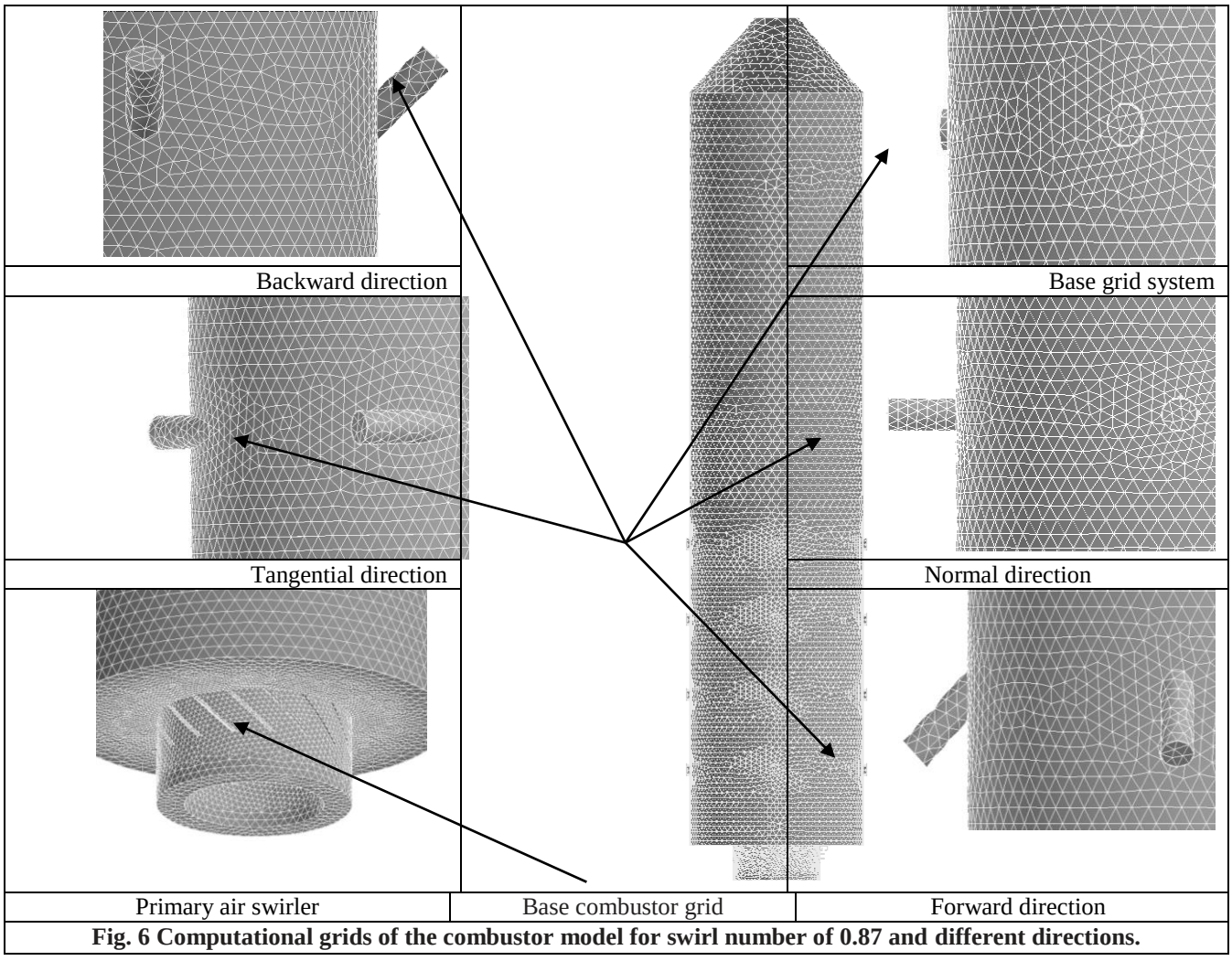

Fig. 6 Computational grids of the combustor model for swirl number of 0.87 and different directions.

The Semi Implicit Method for Pressure Linked Equations (SIMPLE) algorithm was used for pressure/velocity coupling. This algorithm satisfies the mass conservation equation by using a relationship between velocity and pressure corrections. Moreover, for the case in hand, where the pressure variation between consequent mesh cells was expected to be significant, the pressure staggering scheme was used. Such scheme computes the staggered pressure values at the face of each cell in order to capture the pressure nonuniformity.

Numerical parameters such as grid size and boundary conditions in the calculation of the 3-D flows are essential. Fine grids are needed to resolve the flow inside a combustor model. Numerical accuracy can be substantially improved by careful distribution of the grid nodes which offers a good compromise between the computational time and the numerical accuracy, removing the need for a more sophisticated grids. Grid density plays an important role in the solution accuracy. Figure 6. Shows the computational grids for the different combustor models used in the present study. The figure includes the grid system for the base combustor and sections of the others for normal, forward, backward, and tangential directions.

As seen from that figure, the generated grid has high density for zones of great interest (the swirler, near wall and secondary air inlets) and low density in zones of less interest so that computational effort can be minimized but keep sufficient accuracy. The inlet boundary conditions are defined as mass flow inlet of primary air while the exit boundary is defined as pressure outlet with zero gauge pressure. In order to obtain a grid-independent solution, the grid should be refined until the solution no longer varies with additional grid. The effect of mesh refinement on the solution was performed for primary air mass flow of 100 g/s and the cell number of the examined meshes are of 175000, 225000, 300000 and 400000, respectively. The solution of the axial velocity along the centerline of the combustor for the studied meshes was performed. There is a good agreement of the axial velocity along the combustor centerline for 300000 and 400000 mesh sizes while the

results from the other two cases are far from this agreement. Therefore, the mesh size of 300000 can provide a sufficiently grid independent and accurate solution.

4. RESULTS AND DISCUSSION

The aim of this paper is to study the flow field inside a gas turbine combustor using different air swirlers, different secondary air inlet directions and different secondary to primary air ratios. In high swirling flows, the adverse axial pressure gradient is sufficiently large to result in reverse flow along the axis and setting up of an internal recirculation zone. This recirculation zone, which has the form of a toroidal vortex, plays an important role in flame stabilization, as it constitutes a well mixed zone of combustion products and acts as a source of heat and chemically active species located near the burner exit. The trace of points that have zero axial velocity divides the flow field into two flow zones with respect to the flow direction. Forward flow zone, and reverse flow zone (RFZ) are performed. The trace of these points is named as boundary of the RFZ. The boundary of the RFZ is detected by a flow direction detector probe [17]. In the present study, the primary air swirl number was changed by using four air swirlers having the same dimensions but differ in the swirler vane angles.

The size of the recirculation zone is slightly larger than that of the RFZ. So, the two zones can be considered almost the same. [1]. The RFZ for open end and restricted end combustors are shown in Fig. 7, a and b, respectively. For S=0.23, a RFZ of small size was found which takes the shape of ellipsoid and is nearly the same for the open and restricted end combustors. Fig. 7, shows the results from the CFD computations which are compared with test data for verifying the model. Predictions from sst k-ω model presented a good agreement with the experimental data.

For swirl number of 0.5, 0.87 and 1.5 and for open end combustor, the size of the RFZ increases in diameter with the axial distance from the air swirler and reached a maximum diameter, then decreased at further axial distance. Because the combustor is being opened, the size is slightly increased near the combustor exit. In this case, the RFZ boundaries fill the combustor.

For the restricted end combustor and for swirl numbers of 0.5, 0.87 and 1.5, the RFZ sizes are decreased due to the effect of end restriction. The RFZ takes the shape of closed loop, i., e., the RFZ ended inside the combustor. This is because the combustor end restriction helps to diminish the outside air from entering the combustor flow inside. Therefore, the combustor must be have end restriction to make the RFZ end (ellisoid shape) inside the combustor. It is shown that, as the swirl number increases, the size of the RFZ is increased. This is happened in both cases; for open end and restricted end combustor. Also, as the swirl number increases, the bottom of the RFZ is more attached to the combustor upstream.

From computations, the axial velocity components displayed on a centerline plane are presented in Figs. 8-10. The velocity distributions are represented as velocity maps (filled contours of velocity range). The velocity maps are obtained by representing the velocity ranges by colored regions. The axial velocity maps for different swirl numbers at SPAR=0 are presented in Fig. 8. The boundary of the black region represents the boundary of the RFZ. From the figure it is shown that the size of the RFZ is increased in length and diameter as the swirl number increases. The levels of the reversed flow velocity inside the RFZ is increased while the levels of the forward flow velocity outside it decreases as the swirl number increases.

Figure 9 shows the axial velocity distributions for different SPAR [S=0.87& normal direction]. The case of SPAR=0 is presented at the left in order to facilitate the comparison. It is clear that the axial velocity distribution and the size of the RFZ are not affected when introducing secondary air with SPAR=0.25 while the RFZ size is remarkably decreased as SPAR is further increased.

The effect of secondary air direction on the axial velocity distribution and the RFZ is shown in Fig. 10. The RFZ for different directions are arranged according to the decrease in their sizes. The RFZ for SPAR=0 has the largest size. The RFZ in case of forward direction is slightly decreased while it is further decreased due to the effect of normal direction where the axial velocity levels, inside its reverse flow region is smaller than that of forward direction. Therefore, the secondary air with normal direction is more effective and stronger to diminish the size of the RFZ.. The RFZ for backward direction is smaller than that for forward direction because the reverse axial velocity for backward direction is larger. In case of tangential direction, the RFZ is nearly the same as backward but it has lower reversed axial velocities. Backward direction is opposite to the main flow while tangential direction has same effect as backward for the axial velocity but differs in the swirling effect. The velocity distribution inside the RFZ is important in terms of keeping the combustion gases at low velocity that acts as heat source for fresh air-fuel mixture.

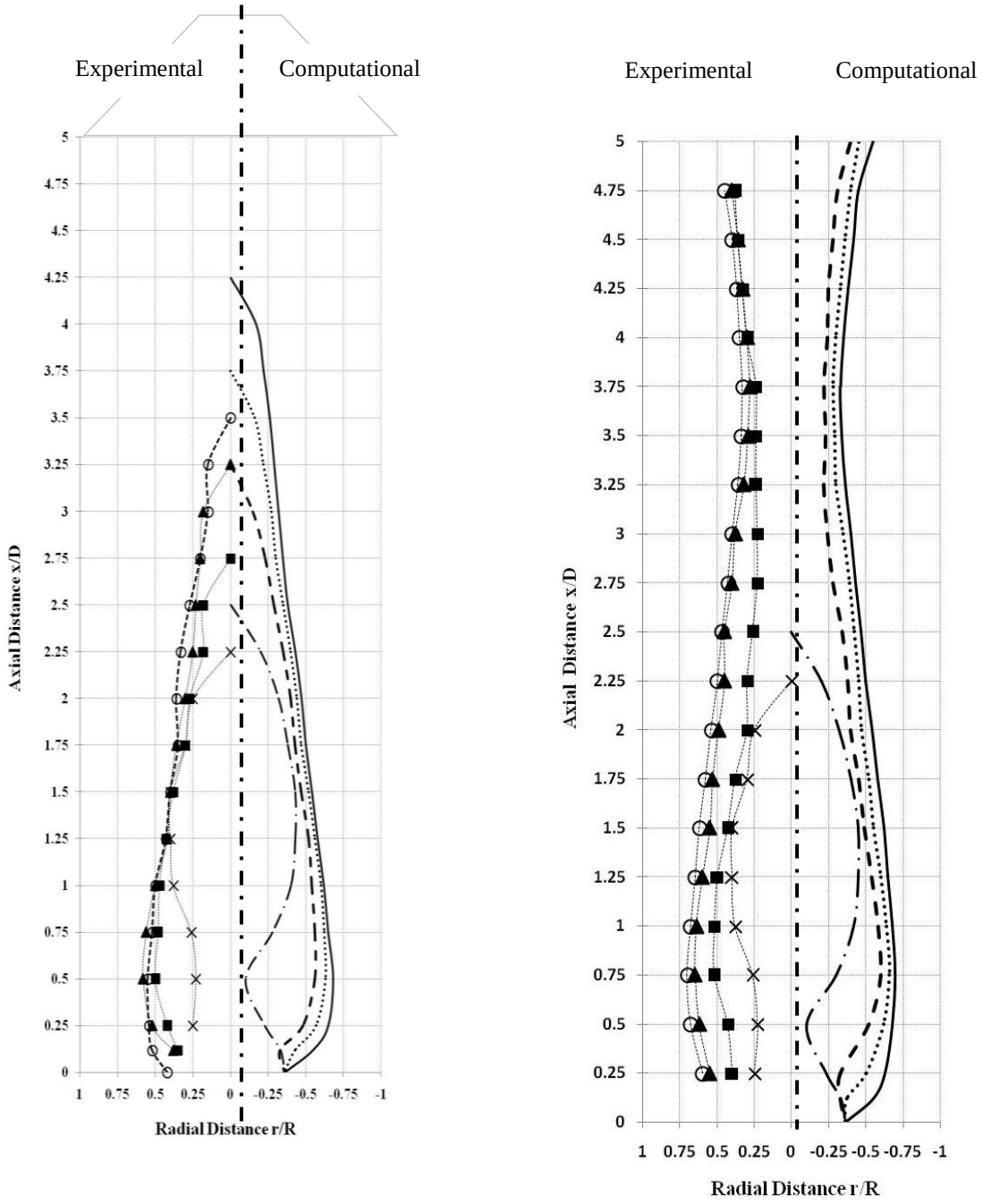

S=1.50, exp.	S=1.50, th.
S=0.87, exp.	S=0.87, th
S=0.50, exp.	S=0.50, th.
S=0.23, exp.	S=0.23, th.

b-Restricted end combustor **a- Open end combustor**

Fig.7.Comparison between the measured RFZ boundaries with that of the computational one at different swirl numbers, for open end and restricted end combustors.

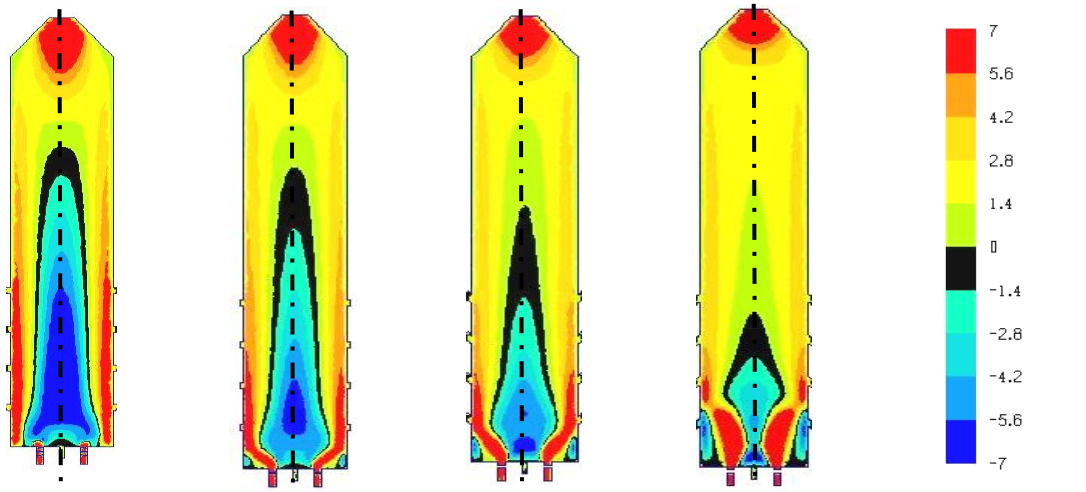

S=1.5 S=0.87 S=0.50 S=0.23 m/s

Fig. 8 Axial velocity distributions for different swirl number at SPAR=0

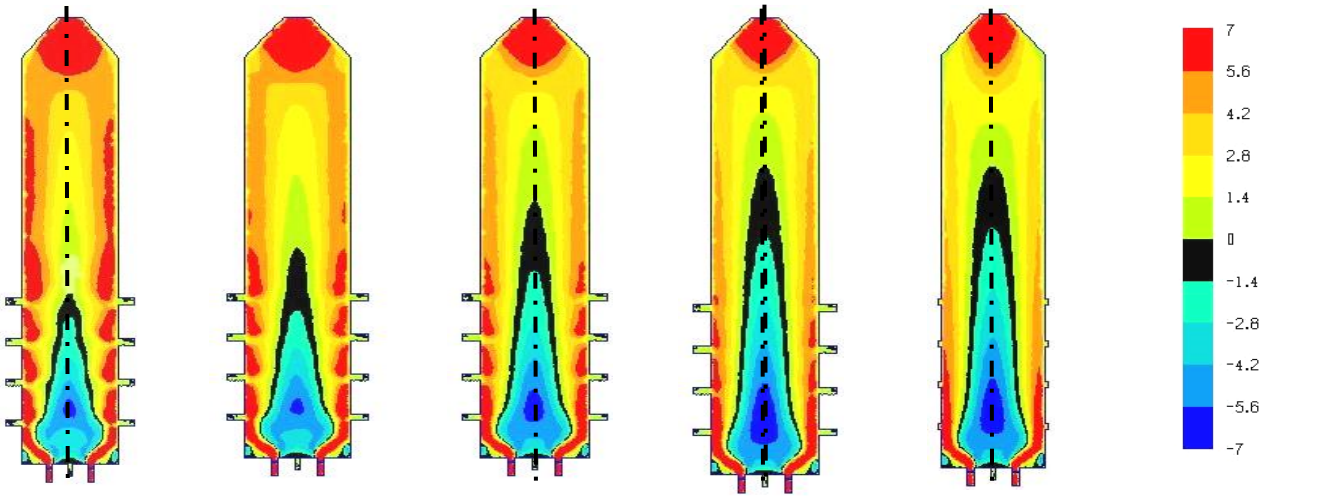

SPAR=1.0 SPAR=0.75 SPAR=0.50 SPAR=0.25 SPAR =0 m/s

Fig. 9 Axial velocity distributions for different SPAR for normal secondary air direction and S=0.87

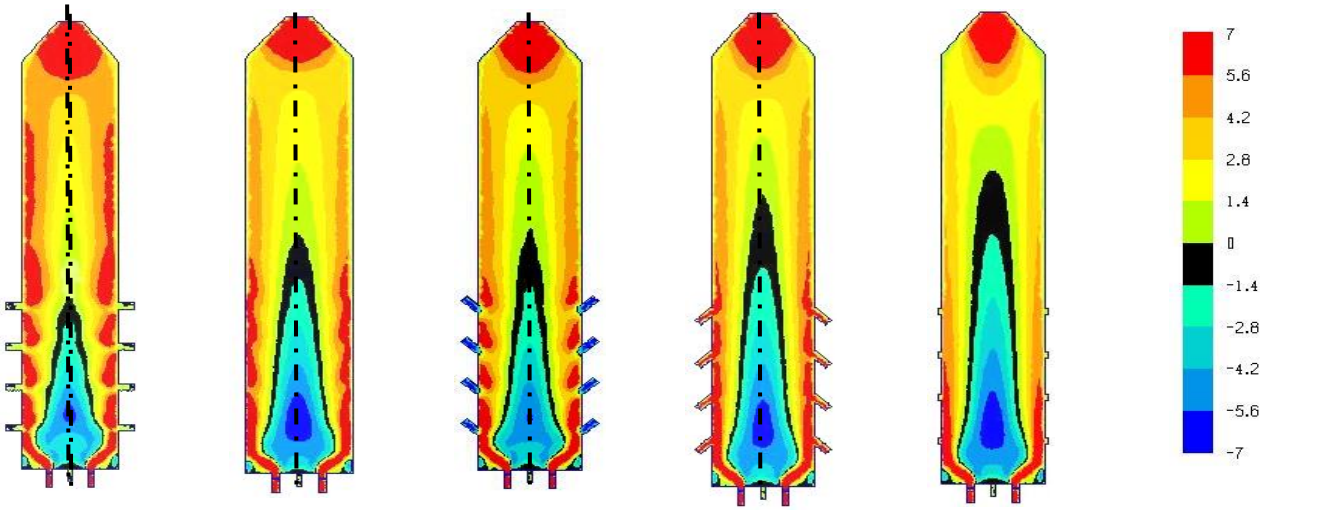

Normal Tangential Backward Forward Base combustor m/s

Fig.10 Axial velocity distributions for different secondary air directions for SPAR=1.0 and S=0.87

From computations, the axial velocity distributions are displayed on planes normal to the combustor centerline, at different axial locations. From the axial velocity distribution inside the RFZ, the recirculated air flow mass ratios can be calculated and plotted at axial locations for different operating conditions. The effect of swirl number, SPAR and secondary air directions on the recirculated air flow mass ratio are shown in Figs. 11, 12 and 13, respectively.

Figure. 11 shows the recirculated mass ratio for different swirl numbers, at different axial locations. The recirculated mass ratio is increased due to the increase in swirl number. For $S \geq 0.5$, this ratio is decreased with the axial distance from the swirler exit. For S=0.23, this ratio is a small value, increased at axial distance equals nearly unity, then decreased again. Figure 12 shows the axial distribution of the recirculated air mass ratio for different SPAR, using normal direction and S=0.87. This ratio is decreased as SPAR is increased resulting in obtaining stable flames.

Figure 13 shows the effect of secondary air direction on the axial distribution of the recirculated air flow mass ratio. The recirculated mass ratio levels are shown for forward, normal, backward and tangential directions which has a higher value levels at SPAR=0 and relatively lower values at SPAR=1.

It is also important to study the turbulence behavior, as well. Figure. 14 shows the percentage turbulence intensity for different swirl numbers. Turbulence intensity levels are increased with increasing the swirl number. Turbulence is produced in the shear layer between the RFZ and the surrounding forward flow and serves to enhance mixing. The highest turbulence intensity is achieved at the maximum tangential velocity, which reveals the conjunction of turbulence with the RFZ formation and its quality. The locus of maximum turbulence intensity can also be of significance in explaining how the tangential and axial flow intercept. When the tangential velocity is maximum, it intercept with the axial flow stream just at the swirler outlet.

Figure. 15 shows the turbulence intensities for different SPAR using normal direction and S=0.87. The reference case of SPAR=0 is presented at the left for comparison. Turbulence levels are increased with increasing SPAR. Turbulence levels are affected by the secondary air direction as shown in Fig. 16. The Highest degree of turbulence is achieved by using tangential direction due to its higher swirling effect. The lower intensity levels occur with the normal direction.

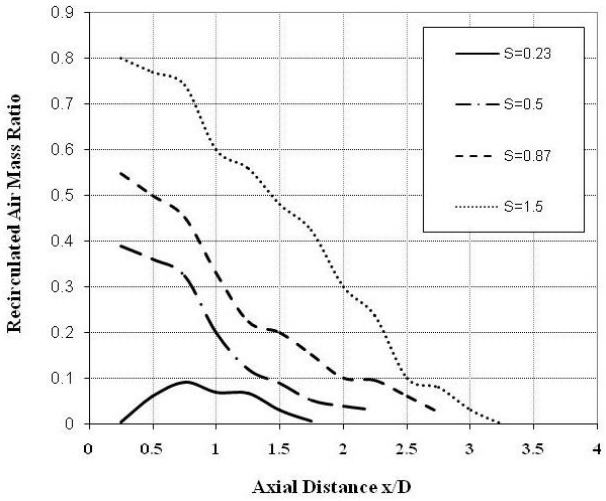

Fig. 11 The axial distribution of the recirculated air flow mass ratio for different swirl numbers of 0.23, 0.5, 0.87 and 1.5 [SAPR=0]

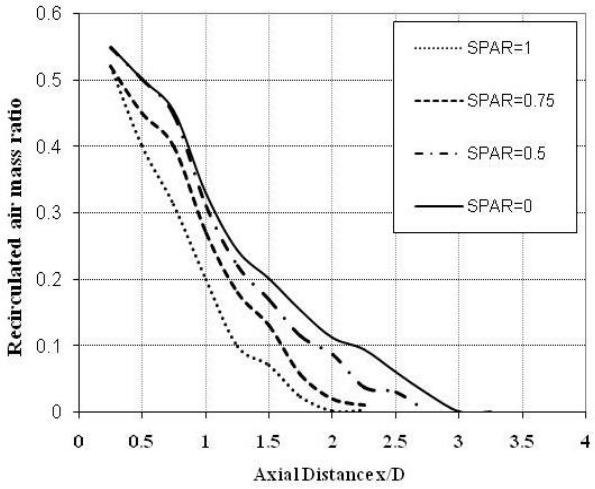

Fig. 12 The axial distribution of the recirculated air flow mass ratio for different SPAR [Normal direction & S=0.87]

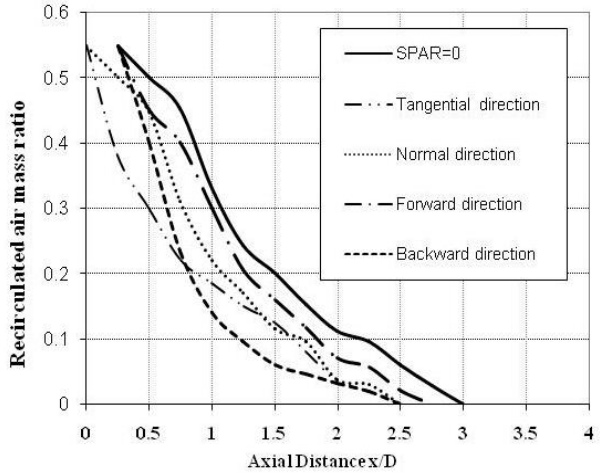

Fig. 13 The axial distribution of the recirculated air flow mass ratio for different secondary air directions [S=0.87 & SPAR=0.5]

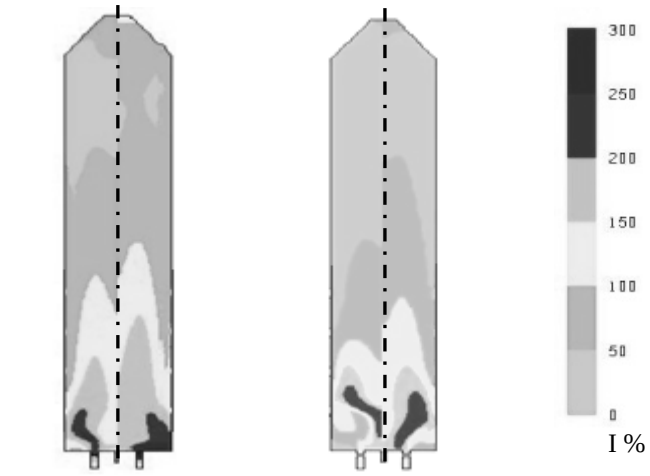

S=1.5 S=0.87 S=0.50 S=0.23

Fig. 14 Percentage Turbulence intensities for different swirl numbers [SPAR=0]

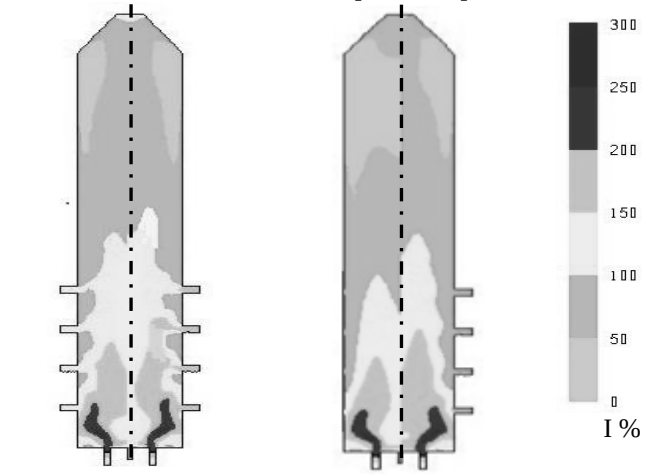

SPAR=1 SPAR=0.75 SPAR=0.5 SPAR=0

Fig. 15 Percentage Turbulence intensities (I) for different SPAR [S=0.87 & normal direction]

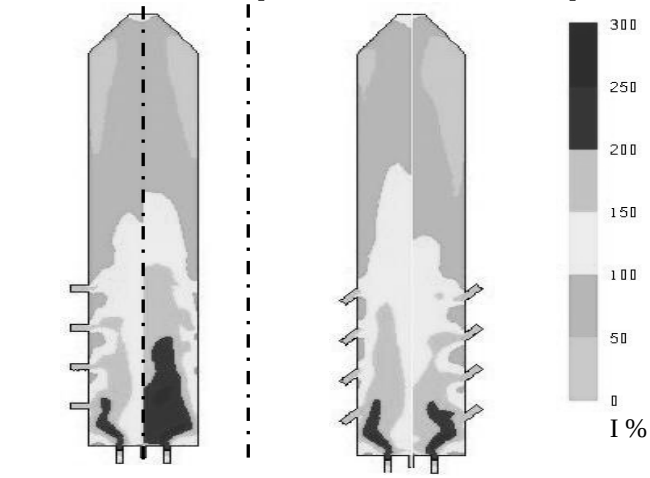

Tangent. Normal Backward Forward

Fig. 16 Percentage Turbulence intensities (I) for different secondary air directions [SPAR=1.0 & S=0.87]

5.CONCLUSIONS

From the computations using the sst k-ω model, the following conclusions are obtained:

1 Comparing the measured and calculated RFZ sizes, good agreement is found

2 Using the combustor restricted end, the boundaries of the RFZ for different swirl numbers up to 1.5, and without secondary air are performed inside the combustor resulting in no air enters the combustor end from outside.

3 Increasing the swirl number, the size of the RFZ is also increased in its length and width. As the swirl number increases from 0.5 up tp 1.5, the length and width of the RFZ are increased by about t 170% and 150%, respectively.

4 Increasing the swirl number and without using secondary air, the axial velocity components are also increased and accordingly the reversed air mass flow rate is also increased and therefore a stable flame is predicted.

5 Increasing SPAR for normal direction at given swirl number, the RFZ size is decreased and also the axial velocity components decreased and accordingly the reversed air flow rate decreases.

6 Using the secondary air for SPAR=1 and S=0.87, the normal direction has the smallest size of the RFZ. The size of the RFZ for forward direction is larger than that of backward one.

7 Increasing the swirl number (at given direction) the recirculated air flow mass ratio also increased while increasing the SPAR (at given S=0.87), it decreased. The recirculated air mass ratio has the higher and lower values for forward and backward directions, respectively.

8 Increasing the swirl number and the SPAR, the turbulence intensity level also increased. This level is higher for tangential direction than the other ones.

REFERENCES

[1] Syred, N., and Beer, J.M., "Combustion in Swirling Flow: A Review", Combustion and Flame, 23:143-201 (1974).

[2] Chigier, N. and Chervinsky, A., "Experimental Investigation of Swirling Vortex Motion in Jets," *Journal of Applied Mechanics*, Vol. 34, 1967, pp. 443-451.

[3] Eldrainy Y.A., Ridzwan J.M.M,, and Jaafar M.N.M., Prediction of the flow inside a micro gas turbine combustor, Jurnal Mekanikal (No 25) (2008) 50–63.

[4] Eldrainy Y.A. Ibrahim M.F.A., and Jaafar M.N.M., Investigation of radial swirler effect on flow pattern inside a gas turbine combustor, Modern Applied Science 3 (5) (2009) 21–31.

[5] Buckley, P.L., Craig, R.R., and Schwartzkopf, K. G., "The Design and Combustion Performance of Practical Swirlers for Integral Rocket/Ramjets", AIAA, 21:733-740 (1983).

[6] Kilik, E., "Better Swirl Generation by using Curved Vane Swirlers", AIAA, 23th Aerospace Sciences Meeting, Reno, 85-1087 (1985).

[7] Kilik, E., "Influence of the Blockage Ratio on the Efficiency of Swirl Generation with Vane Swirlers", AIAA, 85-1103 (1985).

[8] Nejad A. S. and Ahmed S. A, "Flow field characteristics of an axisymmetric sudden-expansion pipe flow with different initial swirl distribution" Int. J. Heat and Fluid Flow, Vol 13, No. 4, (1992)

[9] Ahmed, S.A., and Nejad, A.S., "Velocity Measurements in a Research Combustor. Part I: Isothermal Swirling Flow", Experimental Thermal and Fluid Science Journal, 5:162-174 (1992).

[10] Sheen, H.J., Chen, W.J., and Jeng, S.Y., "Recirculation Zones of Unconfined and Confined Annular Swirling Jets", AIAA, 34, No. 3:572-579 (1996).

[11] Mathur, M.L., and Maccallum, N.R.L, "Swirling Air Jets Issuring from Vane Swirler. Part 2: Enclosed Jets", Journal of the Institute of Fuel, 40:238-245 (1967).

[12] Syred, N., and Dahman, K.R., "Effect of High Levels of Confinement Upon t he Aerodynamics of Swirl Burners", Journal of Energy, 2:8-15 (1978).

[13] Fu, Y., Cai, J., Jeng, S.M., and Mongia, H., "Confinement Effects on the Swirling Flow of a Counter-Rotating Swirl Cup" Proceedings of GT 2005, 238-245

[14] Syred, N., Chigier, N.A., and Beer, J. M., "Flame Stabilization in Recirculation Zones of Jets With Swirl", 13th Symposium (international) on Combustion, The Combustion Institute, 617-624 (1971).

[15] Attya, A. M., Habib, M. A., and Taha, M. R., "Flow and mixing in a gas turbine combustor", the Bulletin of Faculty Eng., Cairo Univ., Egypt, PP. 419-438, (1990).

[16] Tsioumanis N., Brammer J. G. and Hubert J., "Flow processes in a radiant tube burner: Isothermal flow", Fuel 87 (2008) 103–111

[17] Thundil K.R., and Ganesan, V., "Study on the Effect of Various Parameters on Flow Development Behind Vane Swirlers", Int. Journal of Thermal Sciences 47:1204–1225 (2008).

[18] Farag, T.M., "Reverse Flow Zone Measurement in a Swirl Combustor Model", PSEJ, Suez Canal University, 6:120-137 March (2002).

[19] Gad H. M., Farag T. M., Abdel-Mageed S. I., Habik S.E. and Ezz-Eldien A. H." Kerosene spray combustion characteristics in a swirl type combustor with normal secondary air", PSERJ, Volume 14, No. 2, September 2010, pp. 52 - 66

[20] FLUENT 6.3 User's Guide, Fluent Inc., September, 2006.

[21] GAMBIT Program User Guide, September (2006).

[22] Menzies K.R., "An evaluation of turbulence models for the isothermal flow in a gas turbine combustion system" 6th International Symposium on Engineering Turbulence Modeling and Experiments, Sardinia, Italy, 2005.

[23] Nasser Shelil, "Flashback Studies with Premixed Swirl Combustion", Ph. Dr. Dissertation, Cardiff School of Engineering, Cardiff University, UK 2009